Long-term field monitoring of fatigue cracks for steel bridges with wireless large-area strain sensors

Taher, Sdiq Anwar, Li, Jian, Jeong, Jong-Hyun, Laflamme, Simon, Jo, Hongki, et al.

Sdiq Anwar Taher, Jian Li, Jong-Hyun Jeong, Simon Laflamme, Hongki Jo, Caroline Bennett, William Collins, Han Liu, Austin Downey, Mona Shaheen, "Long-term field monitoring of fatigue cracks for steel bridges with wireless large-area strain sensors," Proc. SPIE 12046, Sensors and Smart Structures Technologies for Civil, Mechanical, and Aerospace Systems 2022, 1204604 (18 April 2022); doi: 10.1117/12.2613072

SPIE.

Event: SPIE Smart Structures + Nondestructive Evaluation, 2022, Long Beach, California, United States

Long-term Field Monitoring of Fatigue Cracks for Steel Bridges with Wireless Large-Area Strain Sensors

Sdiq Anwar Taher [1], Jian Li [1*], Jong-Hyun Jeong[2], Simon Laflamme[3], Hongki Jo[2], Caroline Bennett[1], William Collins[1], Han Liu[3], Austin Downey[4], and Mona Shaheen[1]

[1]Department of Civil, Environmental and Architectural Engineering, The University of Kansas, Lawrence, KS, USA
[2]Department of Civil, Architectural Engineering and Mechanics, The University of Arizona, Tucson, AZ, USA
[3]Department of Civil, Construction, and Environmental Engineering, Department of Electrical and Computer Engineering, Iowa State University, Ames, IA, USA
[4]Department of Mechanical Engineering, Department of Civil and Environmental Engineering, University of South Carolina, Columbia, SC, USA

ABSTRACT

Steel bridges are susceptible to fatigue damage under traffic loading and many bridges operate with existing cracks. The discovery and long-term monitoring of those fatigue cracks are critical for safety evaluations. In previous studies, the ability of the soft elastomeric capacitor (SEC) sensor that measures large-area strain was validated for detecting and monitoring fatigue crack growth in a laboratory environment. In this study, the performance of the technology is evaluated for field applications, for which an approach for long-term monitoring of fatigue cracks is developed. The approach consists of an integrated system, termed the Wireless Large-Area Strain Sensors (WLASS), for wireless data collection and storage, and an algorithm for monitoring fatigue cracks with bridge response induced by traffic loading. In particular, the WLASS consists of soft elastomeric capacitors (SECs) combined with sensor boards to convert capacitance to a measurable change in voltage and a wireless sensing platform equipped with event-triggered sensing, wireless data collection, cloud storage, and remote data retrieval. A modified crack growth index (CGI) is developed through wavelet transform. Using the measurements from the integrated system, the modified CGI is able to obtain the crack status under impulsive loading events due to traffic. The performance of the developed approach is validated using a steel highway bridge.

Keywords: soft elastomeric capacitor, wireless sensors, large-area strain sensor, fatigue crack monitoring, steel bridges, structural health monitoring, wavelet transform, peak detection, traffic loads

1. Introduction

Monitoring fatigue crack is critical for civil infrastructure such as steel bridges for safety evaluations. Human visual inspection by trained inspectors have been the de facto approach for detecting and monitoring fatigue cracks for bridges. However, human inspection is prone to errors due to the randomness of crack location and small crack size, hence it is highly dependent on inspectors' experience and ability. In recent years, several methods to monitor fatigue cracks have been developed through structural health monitoring (SHM) and non-destructive testing (NDT). Examples include computer vision-based methods through feature tracking for in-plane and out-of-plane fatigue cracks [1, 2]. Advanced acoustic emission was proposed for the monitoring of fatigue crack propagation in steel compact tension specimens and T-section girders [3]. Low-cost Radio Frequency Identification (RFID) was used for crack detection of a concrete building [4]. Utilizing built-in piezoelectric sensor/actuators, a diagnostic technique for monitoring crack growth in metallic structures was proposed [5]. However, high cost, complex installation and data processing algorithms, and measurement noise involved in the aforementioned methods may limit their success in practical applications.

Conventional resistive strain sensors such as foil strain gauges can continuously monitor the structural response at low cost. However, due to their small sizes, these strain gauges cannot easily cover the large surface of potential fatigue crack regions [6, 7]. Thus, different large-area sensors have been proposed to overcome the challenge [6-9]. In particular, the soft elastomeric capacitive (SEC) sensors have been shown to successfully monitor strain over a large area [6]. Moreover, previous researches validated the effectiveness of the large-area strain measured from SEC in fatigue crack monitoring

* Associate Professor; Email: jianli@ku.edu

Sensors and Smart Structures Technologies for Civil, Mechanical, and Aerospace Systems 2022, edited by Daniele Zonta, Branko Glisic, Zhongqing Su, Proc. of SPIE Vol. 12046, 1204604 · © 2022 SPIE · 0277-786X · doi: 10.1117/12.2613072

[10-12]. Specifically, using multiple SECs in the form of a dense sensor array over fatigue crack regions, a data processing strategy was proposed for monitoring high-cycle fatigue cracks in a steel girder-to-cross-frame connection [10, 11]. Further investigations of the SEC were carried out under more complex and realistic conditions [12]. The above studies showed the effectiveness of the SEC for fatigue crack monitoring in the laboratory environment.

This study focuses on long-term monitoring of fatigue cracks for real-world applications, such as steel bridges, by developing an integrated system, termed the Wireless Large-Area Strain Sensors (WLASS), and an algorithm for fatigue crack monitoring. The WLASS consists of the SECs to capture large-area in-plane strain (capacitance change) induced by fatigue cracks, a capacitive sensor board to convert the change of capacitance into a voltage signal, a wireless sensor platform equipped with 4G-LTE capability for automated trigger-based sensing, wireless data transmission, cloud storage, and remote data retrieval. To effectively extract normalized strain amplitude from the capacitance data for the crack growth index (CGI), a data processing algorithm is proposed based on peak detection and continuous wave transform (CWT). The effectiveness of the developed approaches is examined through a long-term deployment on a steel highway bridge.

2. Algorithm for fatigue crack monitoring with WLASS

This section presents the integrated fatigue crack monitoring system, WLASS, to measure large-area strain and the mathematical formulations for monitoring fatigue cracks using data from the WLASS.

2.1 The WLASS

The proposed WLASS consists of the following components: 1) SEC for large-area strain sensing; 2) The Xnode wireless smart sensing platform and capacitance sensor board for trigger-based sensing, wireless data collection, cloud storage, and remote data retrieval; and 3) a data processing strategy for fatigue crack growth monitoring. Each component is described in this section as below.

2.1.1 SEC for large-area strain sensing

The core sensing element of the WLASS is the SEC that measures large-area in-plane strain (capacitive strain) [6]. The SEC is a flexible capacitive strain sensor that is able to convert surface strain change to a change in capacitance. The SEC consists of a dielectric layer sandwiched between two conductive layers working as electrodes, and its mathematical model is formulated as:

$$C = \frac{e_0 e_r A}{h} \tag{1}$$

where A is the sensing area of the SEC, h is the thickness of the dielectric, e_0 is the vacuum permittivity, and e_r is dielectric permittivity. Two copper tapes are attached to the bottom and top conductive layers for capacitance measurement, as shown in Figure 1. More detailed descriptions of the SEC can be found in [6]. In this paper, the SEC with size 76.2 mm × 76.2 mm are considered.

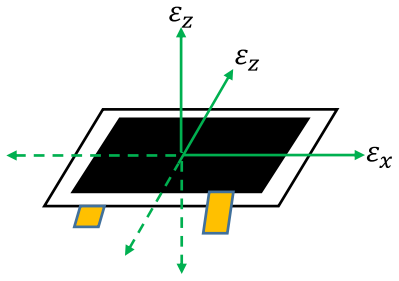

Figure 1. Illustration of the SEC sensor with the principle axes of strains

2.1.2 Xnode wireless sensing platform and capacitance sensor board

This study aims at enabling wireless sensing with the SEC for long-term fatigue crack monitoring in field applications. To this end, the Xnode wireless smart sensor platform [13-16] developed for SHM applications was selected for its flexible

interface with external sensors, reliable wireless communication, high sampling rate and sensing resolution, and rugged design. To enable wireless sensing for the SEC using the Xnode, a capacitance sensor board has been developed [7] based on alternating current (AC) bridge circuit with bridge circuit balancing and Shunt calibration.

The Xnode wireless sensor network contains sensor nodes for sensing and a cellular gateway node with 4G-LTE capability for data transmission, storage, and remote data retrieval. The proposed WLASS is summarized in Figure 2. As illustrated in the figure, the cellular gateway node communicates with sensor nodes to receive measured data and sends it to the cloud server. This capability enables remote data access without physical site visits. Each sensor node has eight channels. The onboard triaxial accelerometers use the first three channels to measure accelerations, while the remaining five channels can be used to measure analog voltage signals from external sensors. Here, those external channels are used to receive voltage signals from the capacitive sensor boards connected with the SEC. As described previously, the capacitive sensor board converts the capacitance obtained from SEC to a measurable change in voltage that falls within the input voltage range of the external channels of the Xnode. The sensor board is designed based on an AC bridge, hence proper bridge circuit balancing and shunt calibration are necessary to ensure accuracy. More detailed description on the sensor board can be found in [7]. As shown in the figure, the C(V) and C(pf) are capacitive strains in terms of voltage and picofarad (pf), respectively. The sensor board receives the 3.3V power supply from the Xnode and measures the capacitance from SEC, while it outputs the capacitance in voltage signal, C(V), to the external channels of the Xnode, which then sends the data to the cellular gateway node. Finally, the cellular gateway uploads the received capacitive strain data, C(V), to the cloud server, which can be accessed using a PC through internet and web browser. Event-triggered sensing mode [15] is employed to collect data through a predefined triggering acceleration threshold. This mechanism ensures only significant loading events are captured, improving power efficiency for long-term fatigue crack monitoring.

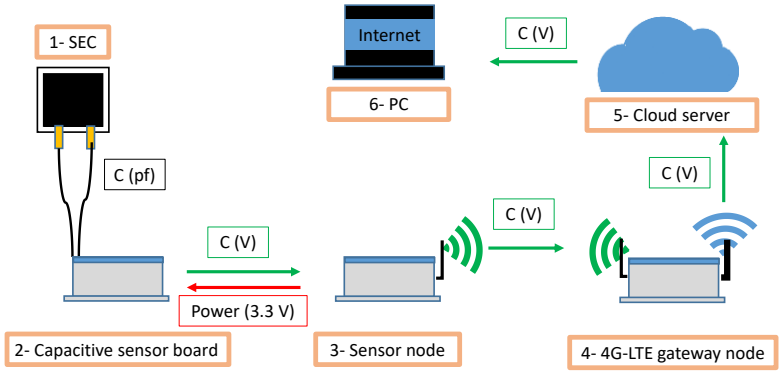

Figure 2. The proposed WLASS for wireless large-area strain sensing, cloud storage, and remote data retrieval

2.2 Algorithm for fatigue crack monitoring

The proposed fatigue crack monitoring algorithm is based on detecting the amplitude of the SEC signal, $C(t)$, under traffic loading to infer crack growth. To remove the impact of the changing load amplitude, a strain gauge is installed at a diagonal member of the cross-frame to indirectly capture the input loading, $F(t)$, that causes distortion-induced fatigue cracks, which is then used to normalize the SEC data ($C(t)$). To this end, the individual impulse events triggered by heavy vehicles are analyzed to extract the amplitude information. Since both the strain and SEC signals, $F(t)$ and $C(t)$, are nonstationary and contain noise and low-frequency drift, to reliably extract their amplitude corresponding to the impulse events, continuous wave transform (CWT) which has been used for non-stationary signals [17] is adopted in this study. CWT decomposes the signal in time-frequency domain, enabling accurate characterization of the signal's changing energy level over time. The formulation of CWT for signal $x(t)$ is [17, 18]:

$$W(t,s) = \int_{-\infty}^{\infty} \frac{1}{s} \varphi^* \left(\frac{\tau - t}{s} \right) x(\tau)\, d\tau \tag{2}$$

where φ is the wavelet function, in which the asterisk indicates the complex conjugate, and t and s are time and scale parameters. In this study, $x(t)$ can be $C(t)$ or $F(t)$, which are the SEC and strain measurements, respectively. Here, the goal is to perform time-frequency analysis of the non-stationary signals based on a wavelet function φ through CWT. In this paper, the generalized Morse wavelets for CWT (GM-CWT) developed in [17-19] is selected for its ability to imply various analytic wavelets by adjusting its parameters. The generalized Morse wavelets is formulated as [17-18]:

$$\boldsymbol{\varphi}_{P,\gamma}(\omega) = U(\omega)\, a_{P,\gamma}\, \omega^{\frac{P^2}{\gamma}} e^{-\omega^{\gamma}} \tag{3}$$

where $U(\omega)$ is the Heaviside step function, $a_{P,\gamma}$ is a normalizing constant, γ and P^2 are the generalized Morse wavelets parameters which control the symmetry and the duration (oscillations) of the wavelet. Various shapes of wavelets can be obtained by adjusting the (γ, P^2) parameters. In this study, the parameters are selected as γ=1.5 and $P^2 = 3$ to extract the amplitudes for the impulse events due to traffic. Note that $W(t,s)$ is a matrix with complex values containing information about the amplitudes of wavelet coefficients. The developed fatigue crack monitoring algorithm includes the following steps:

1. Traffic event detection: The impulse traffic events are detected from the strain data $F(t)$ to obtain the times when the peak strain events occur. Define $\boldsymbol{I} = [I_1, I_2, \dots, I_n]$, $\boldsymbol{F} = [F_1, F_2, \dots, F_n]$, and $\boldsymbol{t} = [t_1, t_2, \dots, t_n]$, in which $\boldsymbol{F}$ and $\boldsymbol{t}$ are the values of the detected peaks and the associated time stored in vectors, $\boldsymbol{I}$ is the indices of the detected peaks stored in vector, and n is the total number of detected peaks. First, local maxima are identified from the time history based on change of derivatives. Then, the local maxima that exceed a pre-defined threshold value are retained as the detected peaks. In this study, the threshold is selected as 30 με. In addition, a minimum peak distance of t_d is also implemented to avoid closely spaced peaks.

2. Wavelet transform and peak identification: $|W(t,s)|_C$ and $|W(t,s)|_F$ are computed for $C(t)$ and $F(t)$ signals, respectively, using the proposed GM-CWT. To identify robust peak values embedded in $|W(t,s)|_C$ and $|W(t,s)|_F$ associated with traffic events for computing the CGIs, windows of interest (WOI) are first defined as $\text{WOI}_i = [t_i - t_d, t_i + t_d]$, where $i = 1,2, \dots, n$. Subsequently, $|W(t,s)|_{C_i}^{max}$ and $|W(t,s)|_{F_i}^{max}$, which are the maximum values of $|W(t,s)|_C$ and $|W(t,s)|_F$, respectively, associated with the detected traffic events are obtained within each WOI_i. Note that $|W(t,s)|_{C_i}^{max}$ is obtained using the index of $|W(t,s)|_{F_i}^{max}$ by assuming the peak events of $C(t)$ and $F(t)$ occur at the same time.

3. The modified CGI: The modified CGI is computed for each peak event as:

$$\boldsymbol{CGI}_i = \frac{|W(t,s)|_{C_i}^{max}}{|W(t,s)|_{F_i}^{max}} \tag{4}$$

The CGI captures the average strain under the SEC sensor normalized by the indirectly measured traffic loading through the cross-frame strain. As a result, changes of CGI can be attributed to potential crack initiation and propagation.

3. Field validation

The developed WLASS was deployed on a steel highway bridge, the 70-105-41732-128 (eastbound) bridge on the I-70 highway near Kansas City, Kansas, as shown in Figure 3a. Multiple locations on the bridge are subjected to fatigue damage and have existing cracks based on the inspection reports provided by the Kansas Department of Transportation (KDOT). A man-lift truck was utilized to access the regions with cracks in the steel girders. In particular, as shown in Figure 3a, the interior side of the exterior girder within Span 3 was selected for instrumentation. A cross-frame was connected to the girder web using a transverse connection plate. As shown in Figure 4, a distortion-induced fatigue crack has been developed near the web-gap region along the weld between the transverse connection plate and the girder web, which has also propagated into the web. This crack is caused by the differential movement between the two adjacent girders. Specifically, the differential displacement results in the out-of-plane force on the girder web by the cross-frame, leading to initiation and propagation of the fatigue crack. Therefore, the diagonal member of the

cross-frame was instrumented with a strain gauge to indirectly infer the level of out-of-plane force demand due to traffic loading (see Figure 3c).

3.1 Measurement setup

The average strain under the fatigue crack is captured by the SEC, while the out-of-plane force demand from the cross-frame is obtained from the strain gauge. To install the SEC and the strain gauge, the surface was first cleaned up. Subsequently, a two-part epoxy, J-B weld was utilized to install an SEC on the crack region of the web, whereas adhesive and coating were applied to install the strain gauge on the cross-frame (see Figure 3c and Figure 4b). Figure 4a and Figure 4b show the surface before and after installing the SEC. The SEC was connected to a capacitive sensor board, which was in turn connected to the Xnode for wireless data collection and remote data retrieval. Note that to ensure robust connections between the capacitive sensor board and the Xnode, a breakout box was used. Moreover, a DC (direct current) Wheatstone bridge was utilized for measurement using the strain gauge. After the installation, AC bridge balancing and Shunt calibration were performed for the capacitive sensor board. The calibration factor was then used to convert the measured voltage signal into capacitance data. Due to limited power supply for the WLASS, including both the sensor node and the 4G cellular gateway, event-triggered sensing mode was used to collect data from significant truck loading through a predefined triggering threshold.

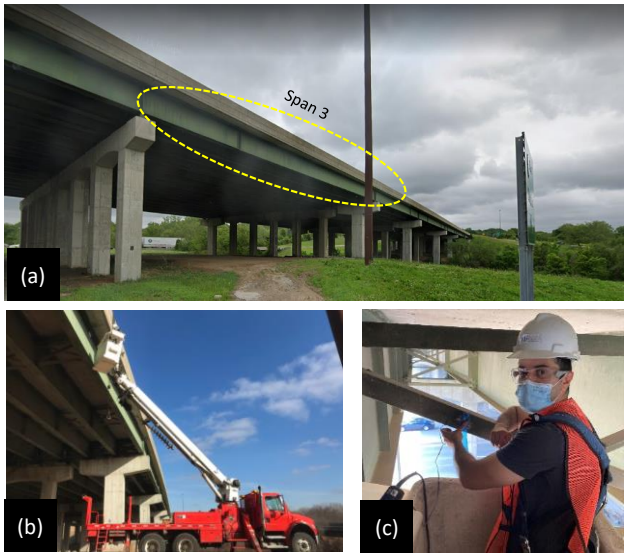

Figure 3: a) The steel highway bridge testbed; (b) a man-lift truck to access the bridge girders; (c) installation of strain gauge

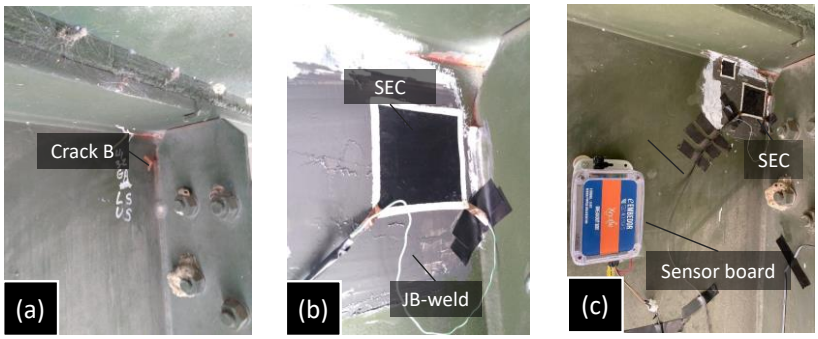

Figure 4: Installation of SEC and the WLASS

3.2 Fatigue crack monitoring

This section demonstrates the data processing results based on the algorithm described in section 2.2 for crack monitoring using the field data over a period of one month.

3.2.1 The GW-CWT results

The proposed approach to extract the signal components of the peak events is verified here. Figure 5a and Figure 6a show typical signals of the large-area strain and the cross-frame strain measurements. The impulse events due to the traffic loading can be clearly seen, demonstrating the effectiveness of the proposed WLASS in capturing the large-area strain and the cross-frame strain for the bridge. Subsequently, as shown in Figure 5b and Figure 6b, the magnitudes of GM-CWT, $|W(t,s)|_c$ and $|W(t,s)|_F$, were calculated for SEC and strain data, respectively. The hot spots in the figures show the concentrated signal energy in both time and frequency domain, which are associated with the impulse traffic events. Figure 8 shows the hot spots for both the large-area strain and the cross-frame strain within the windows of interest (WOIs), which will be described in the next section.

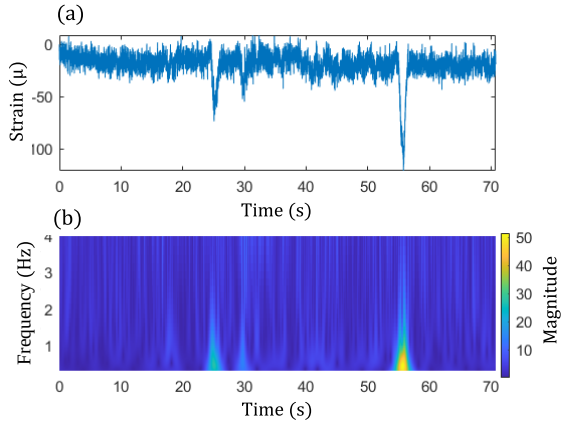

Figure 5. Cross-frame strain measurement from strain gauge under traffic loading: a) raw data, and b) magnitude of GM-CWT coefficient

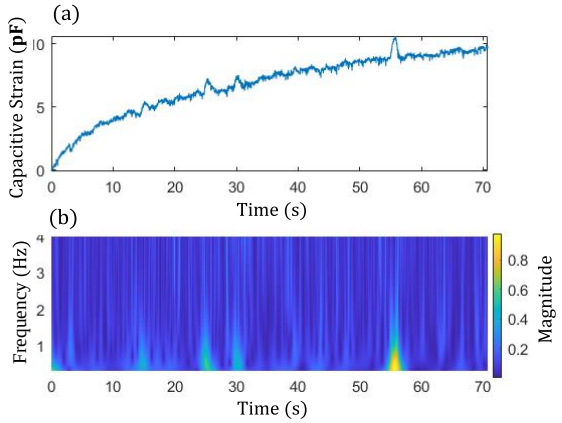

Figure 6. The large-area strain measurement from the SEC near the web gap region: a) raw data and b) magnitude of GM-CWT coefficient

3.2.2 Traffic event detection and WOI

To locate the impulse traffic events for robustly extracting the amplitudes for the GM-CW results, peak detection was performed based on the cross-frame strain measurement shown in Figure 5a. The cross-frame strain was selected for traffic event detection because it indirectly captures the traffic loading and has relatively low noise and clear peaks. The peak detection results will be used to find the WOIs of the magnitudes, $|W(t,s)|_C$ and $|W(t,s)|_F$, for computing the CGIs. To detect peaks, the strain threshold of $h = 30\mu\varepsilon$ and minimum peak distance of $t_d = 1.3s$ were utilized. High-pass and low-pass filters were used to remove the low frequency drift and high frequency noise in the strain signal before peak detection. Figure 7 shows the detected peaks (red dots) from the filtered cross-frame signal. With the times of the detected peaks, t_i, the WOIs were obtained as $[t_i - t_d, t_i + t_d]$, which are illustrated in Figure 7 as small circles.

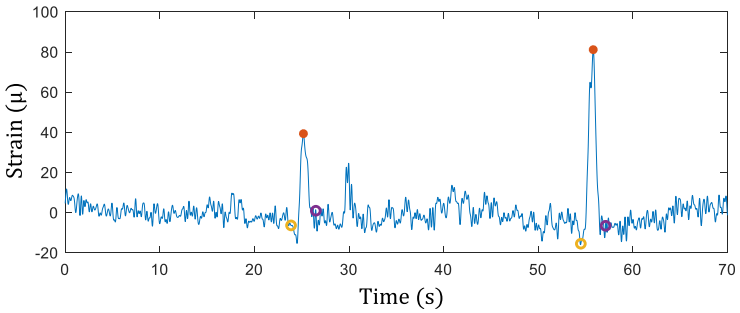

Figure 7. Identified traffic events and WOIs from the strain measurement

Based on the WOIs, the $|W(t,s)|_{C_i}^{max}$ and $|W(t,s)|_{F_i}^{max}$ were extracted within its respective WOI_i, and the results are illustrated in Figure 8. The red solid dots in the figure show the maximum peaks in the cross-frame strain (Figure 8a) and its corresponding peaks in the SEC strain (Figure 8b).

3.2.3 Fatigue crack monitoring result

The fatigue crack monitoring result in terms of the modified CGI using the proposed approach is illustrated here. Data collected during a period of roughly one month is utilized here for demonstrating the field monitoring result, during which the WLASS was triggered for 15 days, leading to a total of 22 datasets. For each dataset, the modified CGIs were obtained using Eq. (4) of each WOI. Figure 9 shows the obtained CGIs over the monitoring period. Specifically, the CGIs obtained during each day was used to compute the mean and standard deviation. The results show that the CGIs remain relatively constant without significant variations, indicating the crack size remained constant during the monitoring period.

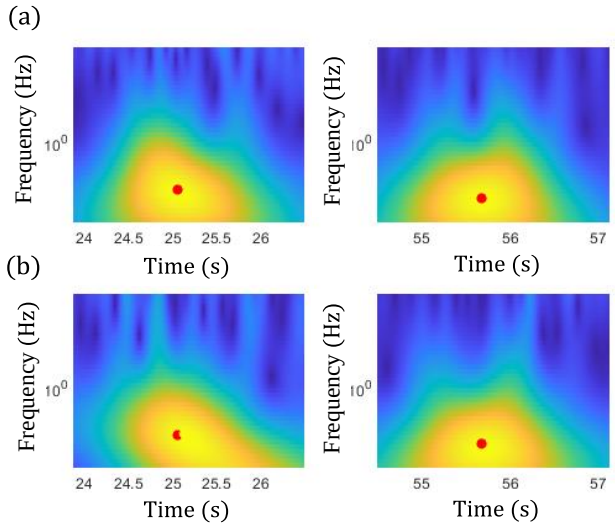

Figure 8 Peak identification within the identified WOIs for a) strain, and b) SEC

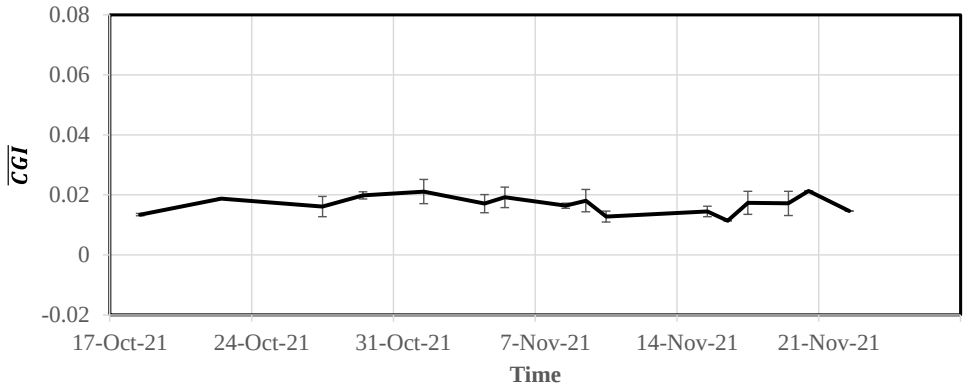

Figure 9. Monitored CGIs (mean and standard deviation) over one month

4. Conclusions

An integrated wireless large-area strain sensor (WLASS) system has been proposed to perform long-term autonomous monitoring of fatigue cracks in steel bridges in this paper. The WLASS consists of the SEC sensor for large-area strain sensing, a capacitive sensor board to covert the capacitance changes of the SEC to measurable voltage signals, a wireless sensing platform for energy efficient trigger-based data collection, cloud storage, and remote data retrieval. Moreover, using the SEC and strain signals, an effective algorithm for fatigue crack monitoring has been proposed to obtain reliable crack growth indices (CGIs) based on traffic induced impulse bridge responses and wavelet transform. In particular, the proposed algorithm consists of traffic event detection, wavelet transform and peak identification, and CGI calculation. A field deployment has been carried out on a steel highway bridge with active distortion-induced fatigue cracks. Data collected during a period of one month has been used to monitoring a fatigue crack near the web gap region. Result showed that the crack size remained constant during the monitoring period.

ACKNOWLEDGMENTS

This research is supported by the Federal Highway Administration (FHWA) Transportation Pooled Fund Study, TPF-5(449), jointly sponsored by the Departments of Transportation of Kansas, Iowa, South Carolina, and North Carolina.

REFERENCE

1. Kong, X., & Li, J. (2018). Vision-based fatigue crack detection of steel structures using video feature tracking. *Computer-Aided Civil and Infrastructure Engineering*, 33(9), 783-799.
2. Taher, S. A., Li, J., Collins, W., & Bennett, C. (2019). UAV-Based Non-Contact Fatigue Crack Monitoring of Steel Structures. *Structural Health Monitoring 2019*.
3. Roberts, T., & Talebzadeh, M. (2003). Acoustic emission monitoring of fatigue crack propagation. Journal of constructional steel research, 59(6), 695-712.
4. Fils, P. D., & Jang, S. (2020, April). Wireless crack detection of a concrete building using low-cost RFID tags. In *Sensors and Smart Structures Technologies for Civil, Mechanical, and Aerospace Systems* 2020 (Vol. 11379, p. 1137904). International Society for Optics and Photonics.
5. Ihn, J. B., & Chang, F. K. (2004). Detection and monitoring of hidden fatigue crack growth using a built-in piezoelectric sensor/actuator network: I. Diagnostics. Smart materials and structures, 13(3), 609.
6. Laflamme, S., Saleem, H. S., Vasan, B. K., Geiger, R. L., Chen, D., Kessler, M. R., & Rajan, K. (2013). Soft elastomeric capacitor network for strain sensing over large surfaces. *IEEE/ASME Transactions on Mechatronics*, 18(6), 1647-1654.

7. Jeong, J. H., Xu, J., Jo, H., Li, J., Kong, X., Collins, W., ... & Laflamme, S. (2018). Development of wireless sensor node hardware for large-area capacitive strain monitoring. *Smart Materials and Structures*, 28(1), 015002.
8. Loh, K. J., Lynch, J. P., Shim, B. S., & Kotov, N. A. (2008). Tailoring piezoresistive sensitivity of multilayer carbon nanotube composite strain sensors. *Journal of intelligent material systems and structures*, 19(7), 747-764.
9. Yao, Y., & Glisic, B. (2015). Detection of steel fatigue cracks with strain sensing sheets based on large area electronics. *Sensors*, 15(4), 8088-8108.
10. Kong, X., Li, J., Collins, W., Bennett, C., Laflamme, S., & Jo, H. (2017). A large-area strain sensing technology for monitoring fatigue cracks in steel bridges. *Smart Materials and Structures*, 26(8), 085024.
11. Kong, X. (2018). Monitoring Fatigue Cracks in Steel Bridges using Advanced Structural Health Monitoring Technologies (Doctoral dissertation, University of Kansas).
12. Kong, X., Li, J., Bennett, C., Collins, W., Laflamme, S., & Jo, H. (2019). Thin-film sensor for fatigue crack sensing and monitoring in steel bridges under varying crack propagation rates and random traffic loads. *Journal of Aerospace Engineering*, 32(1), 04018116.
13. Spencer Jr, B. F., Park, J. W., Mechitov, K. A., Jo, H., & Agha, G. (2017). Next generation wireless smart sensors toward sustainable civil infrastructure. *Procedia engineering*, *171*, 5-13.
14. Hoang et al. (2020). Autonomous end-to-end wireless monitoring system for railroad bridges. Advances in Bridge Engineering volume 1, Article number: 17 (2020)
15. Fu, Y.; Hoang, T.; Mechitov, K.; Kim, J.R.; Zhang, D.; Spencer, B.F., Jr. Sudden Event Monitoring of Civil Infrastructure Using Demand-Based Wireless Smart Sensors. *Sensors* 2018, 18, 4480.
16. Jo, H., Park, J. W., Spencer, B. F., & Jung, H. J. (2013). Develoment of high-sensitivity wireless strain sensor for structural health monitoring. *Smart Struct. Syst*, 11(5), 477-496.
17. Lilly, J. M., & Olhede, S. C. (2008). Higher-order properties of analytic wavelets. *IEEE Transactions on Signal Processing*, 57(1), 146-160.
18. Lilly, J. M., & Olhede, S. C. (2012). Generalized Morse wavelets as a superfamily of analytic wavelets. *IEEE Transactions on Signal Processing*, 60(11), 6036-6041.
19. Olhede, S. C., & Walden, A. T. (2002). Generalized morse wavelets. *IEEE Transactions on Signal Processing*, 50(11), 2661-2670.